Received: 26 June 2020 | Revised: 15 October 2020 | Accepted: 14 December 2020

DOI: 10.1111/nan.12684

Neuropathology and Applied Neurobiology WILEY

ORIGINAL ARTICLE

Protein homeostasis in LGMDR9 (LGMD2I) – The role of ubiquitin–proteasome and autophagy–lysosomal system

Veronika Franekova[1] | Hilde I. Storjord[2] | Gunnar Leivseth[1] | Øivind Nilssen[1,3]

[1]Department of Clinical Medicine, UiT The Arctic University of Norway, Tromsø, Norway

[2]Department of Pathology, University Hospital of North-Norway, Tromsø, Norway

[3]Department of Medical Genetics, Division of Child and Adolescent Health, University Hospital of North-Norway, Tromsø, Norway

Correspondence
Veronika Franekova, Department of Clinical Medicine, UiT The Arctic University of Norway, 9037 Tromsø, Norway.
Email: veronika.franekova@uit.no

Funding information
This work was supported by Department of Clinical Medicine, UiT The Arctic University of Norway, Tromsø, Norway, the Norwegian Neuromuscular Diseases Foundation (Foreningen for muskelsyke) and the National Advisory Unit on Rare Disorders, Oslo, Norway, project title "Patofysiologiske mekanismer ved Limb Girdle muskeldystrofi type 2I".

Abstract

Aims: Limb-girdle muscular dystrophy R9 (LGMDR9) is an autosomal recessive disorder caused by mutations in the fukutin-related protein gene (*FKRP*), encoding a glycosyltransferase involved in α-dystroglycan modification. Muscle atrophy, a significant feature of LGMDR9, occurs by a change in the normal balance between protein synthesis and protein degradation. The ubiquitin–proteasome system (UPS) and autophagy–lysosomal system play a key role in protein degradation in skeletal muscle cells, but their involvement in the pathology of LGMDR9 is still largely unknown. We have aimed at clarifying whether proteolysis through the UPS and the autophagy–lysosomal pathway is dysregulated in LGMDR9 patients.

Methods: *Vastus lateralis* biopsies from 8 normal controls and 12 LGMDR9 patients harbouring the c.826C>A/c.826C>A *FKRP* genotype were assessed for protein markers related to UPS, the autophagy–lysosomal system and endoplasmic reticulum (ER) stress/unfolded protein response (UPR), followed by ultrastructural analysis by transmission electron microscopy (TEM).

Results: Protein levels of E3 ubiquitin ligases Atrogin-1 and MuRF1 showed a pattern similar to normal controls. Elevation of the autophagy markers Atg7, LC3B-II, decreased level of p62 as well as downregulation of the negative autophagy regulator mTORC1, indicated an activation of autophagy in LGMDR9. Mitophagy markers Bnip3 and Parkin were decreased. TEM analysis demonstrated accumulation of autophagosome-like structures in LGMDR9 muscle. There was also an increase in the expression of ER stress/UPR markers PDI, peIF2α and CHOP and a decrease in IRE1α. However, GRP94, Bip and Calnexin remained unchanged.

Conclusion: Our findings indicate that autophagy and ER stress are induced in LGMDR9 muscle.

KEYWORDS
LGMDR9, LGMD2I, muscle atrophy, UPS, autophagy, ER stress, FKRP

INTRODUCTION

Limb-girdle muscular dystrophy R9 (LGMDR9, also known as LGMD2I) is an autosomal recessive disorder caused by mutations in the gene-encoding fukutin-related protein (FKRP) [1]. FKRP is a ribitol-5-phosphate transferase, which participates in the glycosylation of α-dystroglycan, an important protein link between the extracellular matrix and the cytoskeleton. FKRP deficiency causes insufficient α-dystroglycan glycosylation, resulting in dysfunction of laminin binding and instability of the dystrophin–glycoprotein complex in skeletal muscle [2–4]. Genetic variants in the *FKRP* gene cause a broad spectrum of phenotypes ranging from mild clinical symptoms in LGMDR9 to more severe symptoms seen in congenital muscle dystrophy (MDC1C), Walker-Warburg syndrome (WWS) and muscle–eye–brain disease (MEB), which are also associated with severe brain defects and mental impairment [1, 5]. Dilated cardiomyopathy and ventilatory impairment are common clinical features in these patients [6, 7].

The *FKRP* variant c.826C>A (p.Leu276Ile) is the most frequent cause of LGMDR9 in patients from Northern Europe [8, 9]. The spectrum of LGMDR9 phenotypes ranges from mild calf and thigh hypertrophy with disease onset in the second or third decade to early onset Duchenne-like disease with loss of ambulation in the teens [10]. Prominent proximal muscle weakness and atrophy are significant clinical signs in LGMDR9 [6, 11]. However, the molecular basis underpinning atrophy in LGMDR9 is lacking.

Muscle atrophy occurs by a change in the normal balance between protein synthesis and protein degradation. There are two major proteolytic systems contributing to protein degradation in skeletal muscle – the ubiquitin–proteasome system (UPS) and the autophagy–lysosomal system [12].

UPS degradation is achieved through peptide hydrolysis by the 26S proteasome [13]. The E3 ubiquitin ligases Atrogin-1 (also called MAFbx) and MuRF1 (also known as TRIM63) are important biomolecular markers of the UPS degradation pathway. However, although they have been found to be significantly upregulated in several rodent and human models of atrophy [14, 15], recent reports have indicated that Atrogin-1 and/or MuRF1 might not be chronically upregulated in humans during muscle wasting (reviewed in [16, 17]).

Macroautophagy (hereafter referred to as autophagy) is a highly conserved homeostatic process for lysosome-mediated degradation of cytoplasmic components, including damaged or dysfunctional organelles and toxic protein aggregates [18]. Autophagy can be organelle selective, as demonstrated with mitochondria (mitophagy) [19]. In autophagy, double-membrane-bound vesicles known as autophagosomes sequester cellular components and organelles and fuse with lysosomes where the content of the vesicles is degraded [20]. A certain basal level of autophagy is required for the maintenance of protein homeostasis and muscle mass. Muscle wasting is associated with increased autophagy with excessive autophagosome formation. Suppression of autophagy, on the other hand, results in accumulation of protein aggregates and abnormal organelles, leading to myofibre degeneration [21–24].

Dysfunction in the UPS and/or autophagy has been reported in various muscular dystrophies (reviewed in [25, 26]). However, it is currently unknown if proteolysis through the E3 ubiquitin ligases, Atrogin-1 and MuRF1, and/or the autophagic lysosomal pathway is dysregulated in LGMDR9 patients. Therefore, the purpose of this study was to determine the expression of key markers of UPS, and furthermore, autophagy and its regulatory pathways in LGMDR9 muscle. Skeletal muscle sections were investigated by immunoblot, TEM and indirect immunofluorescence. Protein expression data were correlated with the age of onset, disease duration at biopsy or the level of atrophy in LGMDR9 patients to reveal potential clinical significance.

MATERIAL AND METHODS

Muscle biopsies

Muscle specimens from 12 patients with LGMDR9 (6 males and 6 females, average age at biopsy 25.58 years, range 9–51 years) and from 8 normal controls (4 males and 4 females, average age at biopsy 25.05 years, range 42–65 years) were used in this study. Muscle biopsies were obtained from the *vastus lateralis*, flash frozen in isopentane, cooled in liquid nitrogen and then stored at −80°C for further analysis. All patients affected by LGMDR9 harboured the c.826C>A/c.826C>A *FKRP* genotype and were subjected to investigation in the previous studies [9, 27, 28]. Information concerning age at onset of disease and disease duration was collected via a questionnaire as explained in [9] (Table S1). Additional information about patients can be found in [28].

Antibodies

Primary antibodies

Protein kinase B (PKB/Akt, 9272), phospho-Ser473-Akt (pAkt, 4060), AMP-activated protein kinase α (AMPKα, 2532), phospho-Thr172- AMPKα (pAMPKα, 2535), phospho-Ser79 -Acetyl-CoA Carboxylase (pACC, 3661), Atg 12/5 (4180), Atg7 (8558), Bax (5023), Bcl-2 (4223), Beclin-1 (BECN1, 3495), Bip (3183), BCL2/Adenovirus E1B 19 kDa Interacting Protein 3 (Bnip3, 44060), Calnexin (2679), C/EBP homologous protein (CHOP, 2895), eIF2α (9722), phospho-Ser51- eIF2α (peIF2α, 3398), Grp94 (2104), glycogen synthase kinase 3β (GSK3β, 9832), phospho-Ser9-GSK3β (pGSK3β, 9323), inositol-requiring enzyme 1 α (IRE1α, 3294), mammalian target of rapamycin complex 1 (mTORC1, 2972), phospho-Ser2448-mTOR (2971), Parkin (4211), cleaved PARP (Asp214) (9541), protein disulfide isomerase (PDI, 3501), PSMA5 (2457), PSMB5 (12919), Ubiquitin (Ub, 3933), K48-linkage specific polyubiquitin (K48-Ub, 4289), (all from Cell Signaling Technology, USA), Atrogin-1 (SAB2501208), Muscle Ring Finger1 (MuRF1, SAB2105510), LC3B (L7543), p62/

SQSTM1 used in immunoblot analysis (P0067) (all from Sigma-Aldrich, Norway), p62/SQSTM1 (C-terminus) used in immunofluorescence (GP62-C, PROGEN Biotechnik GmbH, Germany), Lysosome-Associated Membrane Protein 2 (LAMP2) used in immunoblot analysis (sc-18822, Santa Cruz Biotechnology, USA), LAMP2 used in immunofluorescence (ab25631, Abcam, UK) and Tumour necrosis factor receptor (TNFR)-associated factor 6 (TRAF6, ab40675, Abcam, UK).

Glyceraldehyde 3-phosphate dehydrogenase (GAPDH, sc-32233, Santa Cruz Biotechnology, USA) was used as a loading control.

Secondary antibodies

Goat anti-rabbit (7074) and horse anti-mouse (7076) antibody conjugated with horseradish peroxidase (HRP) (both from Cell Signaling Technology, USA) were used in immunoblot analysis. The secondary antibodies used in immunofluorescence analysis were Alexa Fluor 555 goat anti-rabbit, Alexa Fluor 488 goat anti-mouse and Alexa Fluor 647 goat anti-guinea pig (all from Invitrogen, Thermo Fisher Scientific, USA).

Immunoblotting

Snap-frozen muscle specimens were homogenized in ice-cold Tissue Protein Extraction Reagent (T-PER, Thermo Fisher Scientific, USA) supplemented with protease (Complete Mini EDTA free inhibitor cocktail, Roche, Germany) and phosphatase (PhosSTOP, Roche, Germany) inhibitor cocktails. After incubation on ice for 15 min, homogenates were cleared by centrifugation (14,000 g/15 min at 4°C). Protein concentration was determined by using BCA Protein Assay Kit (Bio Rad, Norway). For reducing gel electrophoresis, the samples were added Lithium Dodecyl Sulfate (LDS) loading buffer and NuPAGE Sample Reducing agent as recommended by the supplier (Thermo Fisher Scientific, USA) and heated for 10 min at 75°C. Equal amounts of protein (15 µg) were resolved on 4–12% or 4–20% NuPAGE Bis-Tris gradient gels (Thermo Fisher Scientific, USA) and transferred to PVDF membranes (Immobilon, Millipore, USA). Membranes were blocked in 5% (w/V) non-fat dry milk (Blotting-Grade blocker, BioRad, Norway) /Tris Buffered Saline with Tween 20 (TBST, pH 7.5) for 1 hour at room temperature followed by overnight incubation with specific primary antibodies, washed and incubated with the appropriate HRP-conjugated secondary antibodies for 1 h at room temperature. Proteins were detected by enhanced chemiluminescence (SuperSignal West Dura Extended Duration Substrate, Thermo Fisher Scientific, USA), visualized by molecular imager ImageQuant LAS 4000 (GE Healthcare Life Sciences, UK) and quantified by densitometry using Image Studio Lite software (Li Cor Biotechnology, USA). When needed, membranes were stripped with 0.2 M NaOH and reprobed.

Immunostaining and fluorescence confocal microscopy

Muscle biopsies from control and LGMDR9 patients were frozen in Tissue-Tek O.C.T Compound (Sakura, USA). Subsequently, samples were thawed in 8% (w/V) formaldehyde/PHEM buffer (60 mM Pipes, 25 mM Hepes, 10 mM EGTA, 2 mM MgCl2 pH6.9) and fixed overnight. Samples were then infiltrated with 10% (w/V) gelatin for 1 hour, followed by infiltration in 2.3 M sucrose, mounted on cryo-pins and frozen by immersion in liquid nitrogen. Semi-thin sections (approx. 1 µm) were cut on UC7 cryo-ultramicrotome (Leica Microsystems, Austria), picked up with a mix of 2.3 M sucrose and 2% (w/V) methylcellulose and laid onto poly-L-lysine-coated coverslips.

After blocking muscle sections for 1 hour at room temperature with 3% (V/V) goat serum (Sigma-Aldrich, Norway)/Phosphate-Buffered Saline (PBS), samples were incubated for 1 hour at room temperature with appropriate primary antibodies diluted in 1% (V/V) goat serum/PBS. Controls were included where primary antibodies were omitted. Following primary antibodies, sections were washed in PBS five times for 2 min, incubated with fluorescent Alexa Fluor 488 and Alexa Fluor 647 secondary antibodies diluted in 1% (V/V) goat serum /PBS for 1 hour at room temperature and consequently washed in PBS five times for 2 min. Nuclei were counterstained with 4′,6-Diamidine-2′-phenylindole dihydrochloride (DAPI, Sigma-Aldrich, Norway). Confocal microscopy was performed on an LSM800 confocal microscope (Carl Zeiss Microscopy, Germany) equipped with a 63X NA1.4 plan-apochromatic oil immersion objective. For each sample, 10–12 randomly chosen regions of interest were scanned and analysed in Volocity ver. 6.3 (PerkinElmer) to identify colocalized structures.

Transmission Electron microscopy (TEM)

Muscle biopsies were fixed in McDowell-Trumps fixative, postfixed in 1% (w/V) OsO4 and embedded in Epoxy resin (Agar Scientific Ltd., UK). Ultrathin sections (approx. 70 nm) were double stained with uranyl acetate and lead citrate and examined with Hitachi HT7800 Transmission Electron Microscope (Hitachi, Japan) or Jeol 1010 Transmission Electron Microscope (JEOL Ltd., Japan). Micrographs were taken with XAROSA TEM CMOS camera and RADIUS software or Morada Camera system (Olympus Soft Imaging Solutions, Germany).

Statistical analysis and data presentation

All data are presented as means ±SEM, plotted with GraphPad Prism 5 for Windows (GraphPad Software, USA). Statistical analysis was performed by two-tailed unpaired t-test in Microsoft Excel 2016 (Microsoft Corporation, USA). $p < 0.05$ was considered as significant.

RESULTS

UPS degradation in LGMDR9 muscle

The E3 ubiquitin ligases Atrogin-1 and MuRF1 are important biomolecular markers of the UPS degradation pathway and have been shown to be upregulated in multiple physiological settings of atrophy [13]. To investigate if this would also be the case in LGMDR9, protein levels of Atrogin-1 and MuRF1 were estimated by immunoblot analysis in skeletal muscle from patients and normal controls. Results obtained from LGMDR9 muscle biopsies did not show any significant difference in the expression of these two markers with respect to controls (Figure 1A,B). Moreover, expression levels of Atrogin-1 and MuRF1 did not correlate with the extent of atrophy, age at onset or duration of symptoms in LGMDR9 patients (data not shown). We also assessed the levels of protein ubiquitination as well as α5 (PSMA5) and β5 (PSMB5) subunits of 20S catalytic core of 26S proteasome. Western blot analysis revealed an increase in total ubiquitin content in LGMDR9 muscle biopsies as compared to controls. This was accompanied by a significantly increased expression of β5 (PSMB5) and a trend towards increased expression of α5/PSMA5 ($p = 0.1$). Overall, levels of K48-linked ubiquitination did not differ between LGMDR9 biopsies and controls, however, variability in band patterns and intensities was observed between the two groups (Fig. S1).

Autophagy in LGMDR9 muscle

A number of studies have indicated abnormal regulation of autophagy in various forms of muscular dystrophy (reviewed in [25]). To investigate if the autophagy–lysosomal degradation pathway is dysregulated in LGMDR9, protein expression levels of autophagy markers Atg7, Atg12, Beclin-1, LC3B and p62 were assessed in muscles from LGMDR9 patients and normal controls.

Immunoblot analysis showed significant increase in Atg7 expression in LGMDR9 patients as compared to normal controls, however, no difference in the levels of Atg12 and Beclin1 was observed. The lipidated form of LC3B, LC3B-II, which is generated during autophagosome formation, was highly increased in LGMDR9 muscle, whereas the level of p62, a protein known to be incorporated into autophagosomes and efficiently degraded during autophagy, was significantly decreased. Altogether, the results indicate an activation of autophagy in LGMDR9 muscle (Figure 2A,B).

With the exception of LC3B-II, which showed an inverse correlation with age at onset, there were no obvious relationships between the level of atrophy, age at onset or duration of symptoms in LGMDR9 and the expression levels of the above-mentioned autophagy markers (data not shown).

LC3B/p62/Lamp2 colocalization in LGMDR9 muscle

Increased levels of LC3B-II in skeletal muscle from patients with LGMDR9 could be caused either by autophagy induction or by failure in autophagosomes degradation. During functional autophagy, autophagosomes fuse with lysosomes to form autolysosomes, followed by degradation of autophagosomal cargo. Therefore, in order to gain insight into autophagosome–lysosome fusion in LGMDR9 muscle, the abundance of the common lysosomal marker LAMP2 and its intracellular localization relative to LC3B were investigated. Furthermore, since p62 is a resident of autophagosomes, it was also of interest to verify its localization relative to LC3B. No differences in the levels of LAMP2 were observed between controls and LGMDR9 samples upon immunoblot analysis (Figure 3A,B). Immunofluorescence analysis demonstrated that LC3B-, p62- and LAMP2-positive signals were far more abundant in LGMDR9 muscles as compared to control muscle. LC3B co-localized with both p62 and LAMP2 in LGMDR9 muscle, and to a higher extent than in control muscle (Figure 3C,D). This suggests that the content of autophagosomes/autolysosomes in LGMDR9 is increased.

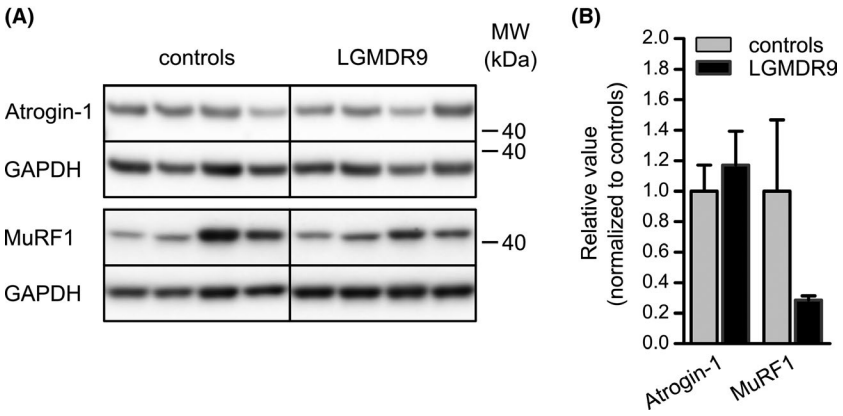

FIGURE 1 UPS in LGMDR9 muscle. (A) Representative immunoblot analyses of muscle biopsies for Atrogin-1, MuRF1 and the loading control GAPDH from normal controls and LGMDR9 patients. (B) Densitometric quantification of the signals from immunoblot analyses corrected for loading control. Quantifications correspond to 8 normal controls and 12 LGMDR9 patients. Results are presented as mean values ±SEM and normalized to normal controls * $p < 0.05$ vs. normal controls

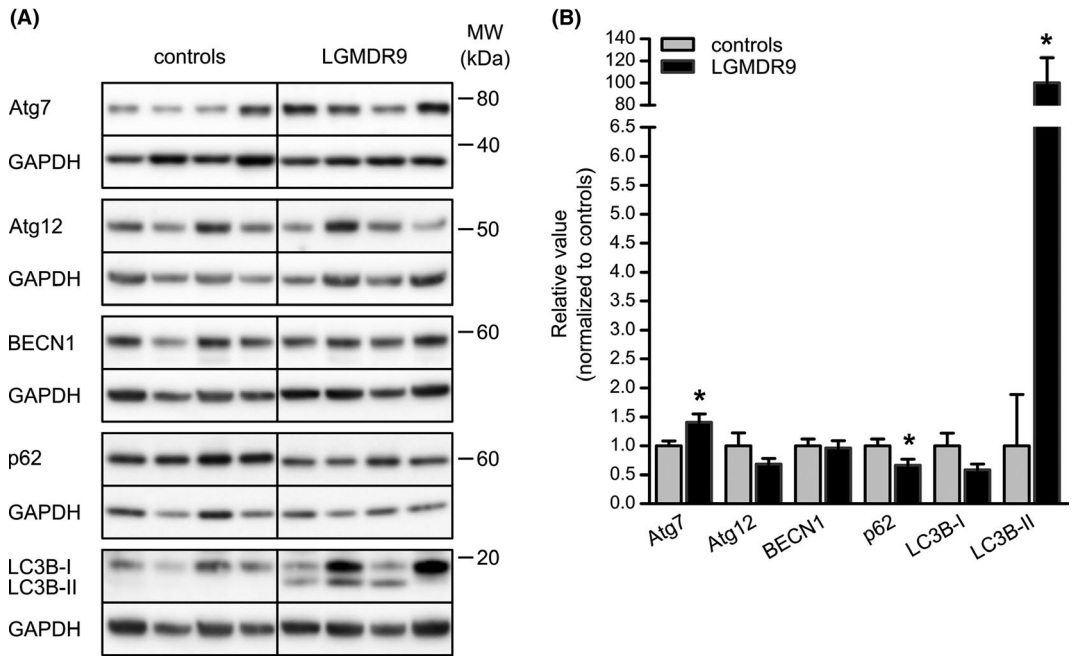

FIGURE 2 Autophagy in LGMDR9 muscle. (A) Representative immunoblot analyses of muscle biopsies for Atg7, Atg12, BECN1, p62, LC3B and the loading control GAPDH from normal controls and LGMDR9 patients. (B) Densitometric quantification of the signals from immunoblot analyses corrected for loading control. Quantifications correspond to 8 normal controls and 12 LGMDR9 patients. Results are presented as mean values ±SEM and normalized to normal controls * $p < 0.05$ vs. normal controls

TEM analysis of LGMDR9 muscle

To further characterize autophagy in LGMDR9 muscle, transmission electron microscopy (TEM) was performed on muscle sections from 11 patients. TEM analysis revealed accumulation of vacuolated structures containing degraded cytoplasmic content and mitochondria. They were observed both within the intermyofibrillar as well as in the subsarcolemmal space of LGMDR9 muscle fibres. Higher magnification revealed that they likely correspond to autophagosomes and autolysosomes (Figure 4A-E, Fig. S2A,B). In addition, fibres contained concentric multi-lamellar structures, highly indicative of an ongoing process of autophagy in LGMDR9 muscle (Fig. S2C,D). Furthermore, morphologically altered mitochondria and dilated sarcoplasmic reticulum (SR) were observed in LGMD2R9 muscles (Figure 4D-G, Fig. S2E-H).

Mitophagy in LGMDR9 muscle

TEM analysis of LGMDR9 muscle sections revealed morphological alterations of mitochondria. Enlarged and swollen mitochondria, mitochondria devoid of cristae and large areas with disintegrated mitochondria were common features of LGMDR9 biopsies. Defective mitochondria can be selectively degraded in the process of mitochondrial autophagy (mitophagy) [29, 30]. Therefore, expression of mitophagy markers, proteins that prime damaged mitochondria and allow the recruitment of the autophagosome for mitophagy, such as Bnip3 and the E3 ubiquitin-protein ligase Parkin (PARK2), was assessed. The results showed significantly reduced expression of Bnip3 and Parkin in LGMDR9 muscle as compared to controls. Notably, a shift towards a higher molecular weight and a smeary pattern of Parkin were detected in LGMDR9 samples (Figure 5).

Regulation of autophagy in LGMDR9 muscle

Akt/mTORC1

Autophagy is regulated by multiple signalling pathways. To elucidate the pathways involved in autophagy enhancement seen in LGMDR9 muscle, the expression and the activation of specific upstream proteins, known to control autophagy, was quantified. Akt/PKB is known to be one of the most potent modulators of autophagy in skeletal muscle, blocking the formation of autophagosomes and the lysosomal degradation of their content [31–33]. Activation of Akt leads to the downstream activation of mTORC1, which besides its stimulatory effect on muscle growth and hypertrophy, also leads to inhibition of autophagy [34, 35]. In addition, Akt phosphorylates and inactivates GSK3β, a positive regulator of autophagy [36, 37]. Therefore, the next step was to determine whether the induction of autophagy observed in LGMDR9 skeletal muscle could be due to diminished Akt signalling.

There were no significant changes in the expression level of total Akt or its activated (phosphorylated) form pAkt (Ser473) in LGMDR9 muscles as compared to those of controls. The level of phosphorylation of mTORC1 (Ser2448) and GSK3β (Ser9), however, was decreased in LGMDR9 muscle as compared to normal controls.

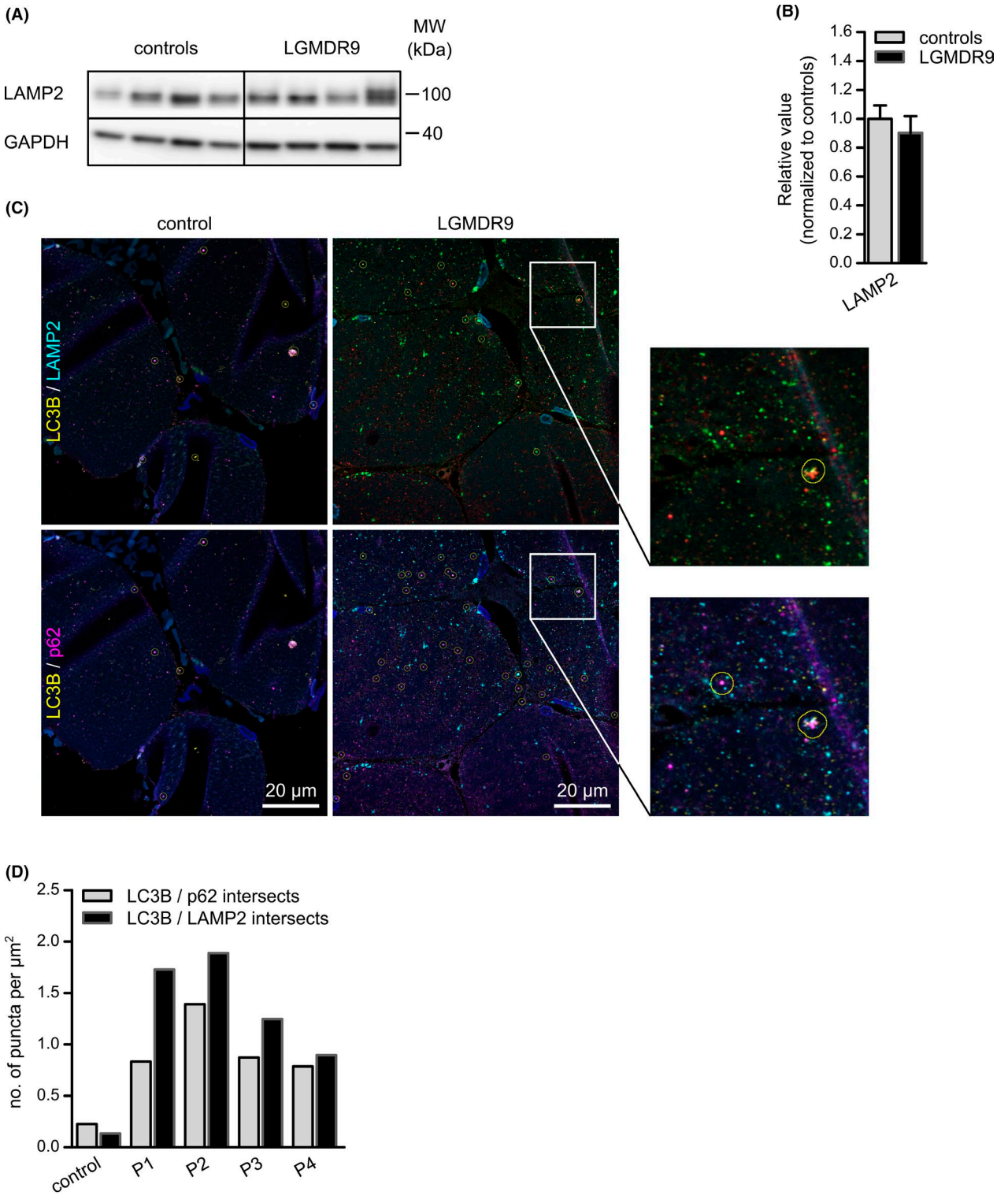

FIGURE 3 LC3B/p62/Lamp2 colocalization in LGMDR9 muscle. (A) Representative immunoblot analyses of muscle biopsies for LAMP2 and the loading control GAPDH from normal controls and LGMDR9 patients. (B) Densitometric quantification of the signals from immunoblot analyses corrected for loading control. Quantifications correspond to 8 normal controls and 12 LGMDR9 patients. (C) Co-immunostainings on cross-sections of muscle biopsies from a healthy control and from a patient with LGMDR9 using antibodies against LC3B (yellow), LAMP2 (cyan) and p62 (magenta) and nuclei counterstained with DAPI (blue). Circled areas denote LC3B/LAMP2 and LC3B/p62 co-localization. (D) Quantification of the fluorescent signals from confocal images from the control (n = 1) and LGMDR9 patients (n = 4)

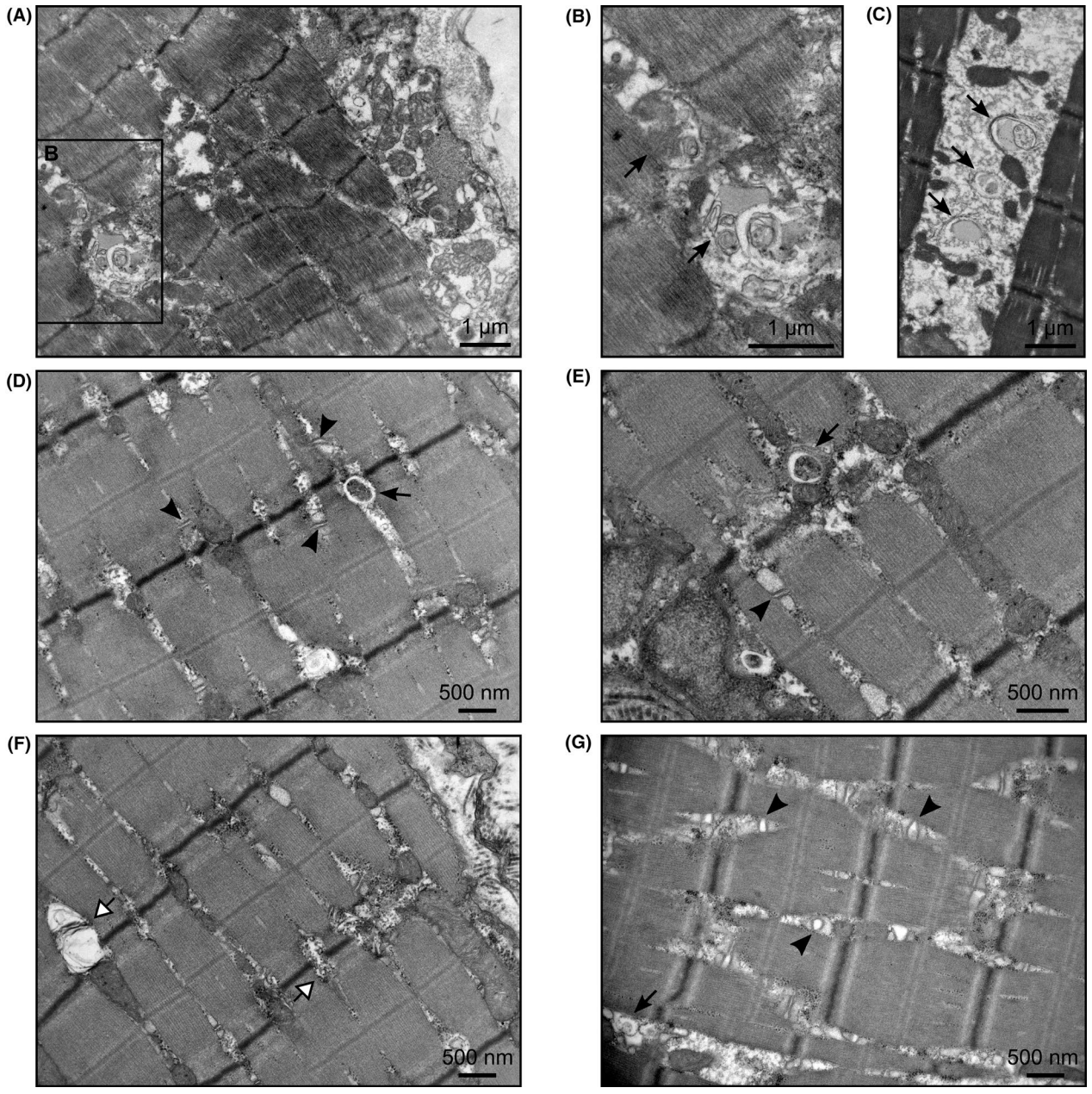

FIGURE 4 Ultrastructural analysis of LGMDR9 muscle. Electron micrographs of *vastus lateralis* muscle biopsies derived from patients with LGMDR9. (A) Low-magnification micrograph showing autophagic vacuoles. (B) Enlargement of autophagic vacuoles and multi-lamellar structures (black arrow). (C) Intermyofibrillar localization of autophagic vacuoles (black arrow) at different stages of autophagy. (D, E) Mitochondria enclosed in an autophagic vacuole (black arrow) and dilated sarcoplasmic reticula (black arrowhead). (F) Swollen mitochondria and disintegrated mitochondria (white arrow). (G) Dilated sarcoplasmic reticula (black arrowhead) and autophagic vacuoles (black arrow)

Likewise, total GSK3β was decreased in LGMDR9 patients when compared to controls (Figure 6).

AMPK and TRAF6

Other proteins involved in the regulation of autophagy independent of Akt signalling are AMPK and TRAF6. AMPK is involved in autophagy activation through inhibition of mTORC1 as well as direct phosphorylation of ULK1, an important factor in autophagy activation [38, 39]. TRAF6 is required for optimal activation of JNK, AMPK, FoxO3 and NF-kB pathways, crucial regulators of autophagy [40]. Previous studies have suggested that muscle-specific depletion of TRAF6 inhibits expression of autophagy-related molecules and autophagosome formation in atrophying skeletal muscle, and that increase in TRAF6 leads to activation of autophagy [40, 41]. Therefore, expression of AMPK and its activated phosphorylated form, as well as TRAF6 were assessed in this study. With regard to the level of phosphorylation of AMPK (Thr172) and acetyl-CoA-carboxylase (ACC-Ser79), another

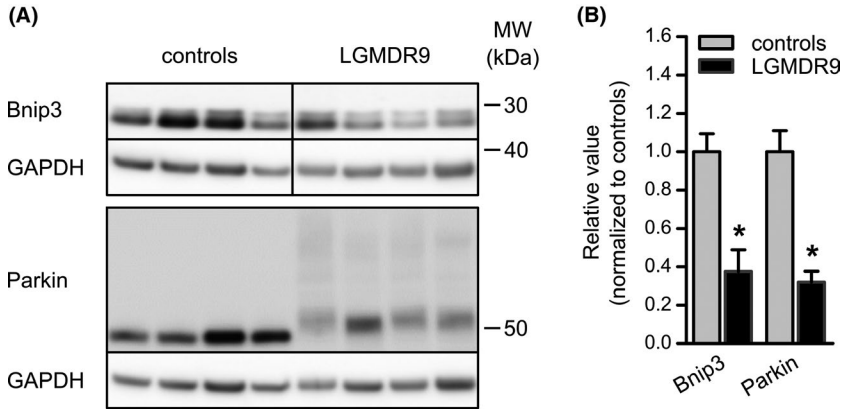

FIGURE 5 Mitophagy in LGMDR9 muscle. (A) Representative immunoblot analyses of muscle biopsies for Bnip3, Parkin and the loading control GAPDH from normal controls and LGMDR9 patients. (B) Densitometric quantification of the signals from immunoblot analyses corrected for loading control. Quantifications correspond to 8 normal controls and 12 LGMDR9 patients. Results are represented as mean values ±SEM and normalized to normal controls * $p < 0.05$ vs. normal controls

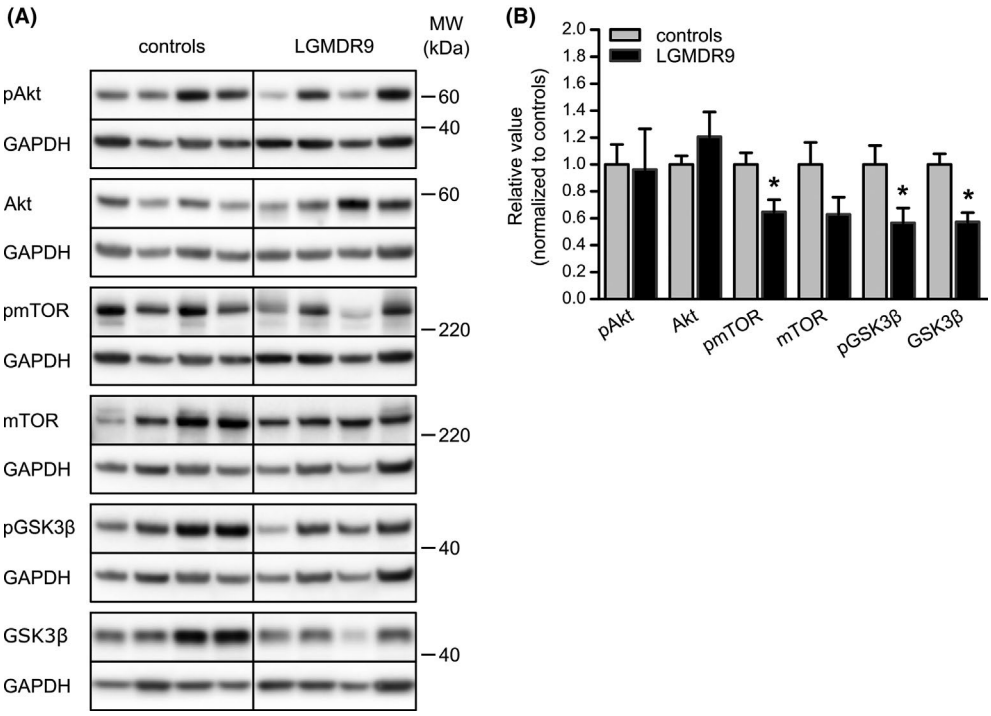

FIGURE 6 Regulation of autophagy in LGMDR9 muscle. (A) Representative immunoblot analyses of muscle biopsies for phospho-Ser473-Akt (pAkt), Akt, phospho-Ser2448-mTOR (pmTOR), mTOR, phospho-Ser9-GSK3β (pGSK3β), GSK3β and the loading control GAPDH from normal controls and LGMDR9 patients. (B) Densitometric quantification of the signals from immunoblot analyses corrected for loading control. Quantifications correspond to 8 normal controls and 12 LGMDR9 patients. Results are represented as mean values ±SEM and normalized to normal controls * $p < 0.05$ vs. normal controls

indicator of AMPK activation, no significant differences between LGMDR9 and control muscles were observed. This was also the case for TRAF6 protein expression (Figure 7).

ER stress/UPR

It has been shown that ER can be a source of membranes during the formation of autophagic vesicles and experimentally generated ER stress can induce autophagy in mammalian cells [42–45]. Several canonical unfolded protein response (UPR) pathways are implicated in this process [44, 46, 47].

In order to assess whether the changes in autophagy seen in LGMDR9 muscle could be due to increased ER stress, expression levels of folding catalysts BiP (also known as Grp78), Grp94, calnexin, PDI, the level of eIF2α, peIF2α (Ser51) and IRE1α, the most conserved ER stress sensor, were measured. With regard to the levels of Bip, Grp94, calnexin and eIF2α, there were no substantial differences in protein expression

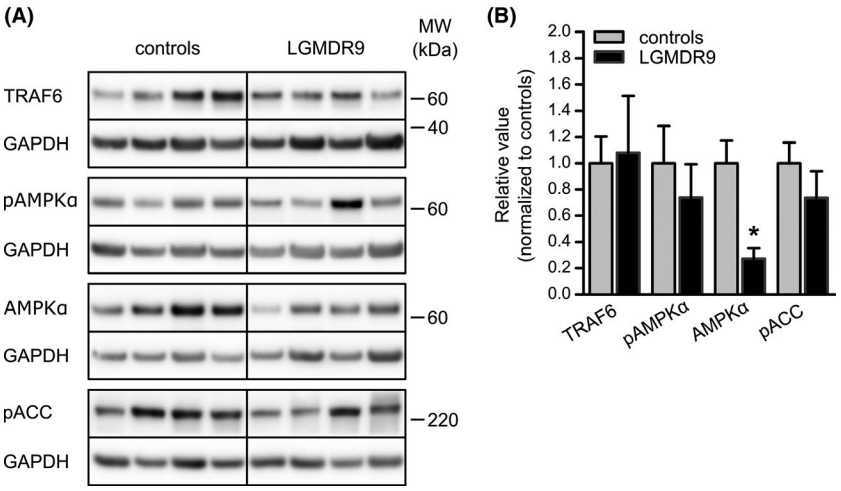

FIGURE 7 Regulation of autophagy in LGMDR9 muscle. (A) Representative immunoblot analyses of muscle biopsies for TRAF6, phospho-Thr172- AMPKα (pAMPKα), AMPKα, phospho-Ser79 -Acetyl-CoA Carboxylase (pACC) and the loading control GAPDH from normal controls and LGMDR9 patients. (B) Densitometric quantification of the signals from immunoblot analyses corrected for loading control. Quantifications correspond to 8 normal controls and 12 LGMDR9 patients. Results are represented as mean values ±SEM and normalized to normal controls $^{*}p < 0.05$ vs. normal controls

between LGMDR9 and control muscles. However, a significant increase in the expression of PDI and peIF2α (Ser51) was found in LGMDR9 muscle when compared to controls. There was also a decrease in the level of IRE1α in LGMDR9 muscle as compared to controls, although it did not reach statistical significance ($p = 0.056$) (Figure 8).

Decreased levels of IRE1α could be a sign of chronic ER stress in patients with LGMDR9. Under prolonged ER stress, UPR signalling can trigger cell death. One major event responsible for this switch between pro-survival and pro-apoptotic responses is the induction of protein CHOP (also known as Growth Arrest and DNA-damage-inducible 153, GADD153) (reviewed in [48]). Significantly increased level of CHOP expression was seen in LGMDR9 skeletal muscle when compared to controls (Figure 8). Moreover, an increase in pro-apoptotic Bax and a decrease in anti-apoptotic Bcl2, both transcriptionally regulated by CHOP, were observed in LGMDR9 samples suggesting an activation of apoptosis in these patients. However, the level of cleaved Parp, another apoptotic marker, remained unchanged (Fig. S3).

DISCUSSION

Several studies have demonstrated an association between dysfunction of the UPS and/or autophagy and the various forms of muscular dystrophy. However, there is no common denominator as some disorders show downregulation and some show activation of the UPS and/or the autophagy–lysosomal system. Upregulation of proteasomal activity as well as an overall increase in ubiquitinated proteins were found in a mouse model (dy3 K/dy3 K) of merosin-deficient congenital muscular dystrophy type I (MDCA1). Likewise, dysregulation of the ubiquitin–proteasome system has also been reported for limb girdle muscular dystrophy (LGMD) types 2H (R8, TRIM32-related), type 2A (D4, calpain3-related) and type 2B (R2, dysferlin-related). Furthermore, markedly reduced mRNA expression of Atrogin-1 and MuRF1 was demonstrated in muscle biopsies of patients with Ullrich congenital muscular dystrophy 1 (UCDM1), whereas no such changes were observed in Duchenne muscular dystrophy (DMD) patients. A dysfunctional autophagic machinery was reported in Collagen VI-related myopathies as well as in DMD. Conversely, increased autophagy flux has been suggested to be involved in muscle atrophy and degeneration in MDC1A as well as in LGMDD4 and LGMDR2 (reviewed in [25, 26]).

LGMDR9 patients are characterized by proximal muscle atrophy. However, the cascade of molecular events leading from the causative *FKRP* mutations to the muscle atrophy is largely unknown. Here, we have examined the role of the UPS and the autophagy–lysosomal system, the two main proteolytic systems associated with atrophy in muscular dystrophy. All LGMDR9 patients included in this study were c.826C>A homozygotes which allowed us to assess changes in different molecular mechanisms on a homogeneous *FKRP* genotypic background.

UPS markers Atrogin-1 and MuRF1 are not upregulated in LGMDR9 muscle

The E3 ubiquitin ligases Atrogin-1 and MuRF1 have been reported to be elevated in a wide range of atrophy-inducing conditions, and thus have become recognized as key markers of muscle atrophy. However, upregulation of these UPS markers seems not be an universal finding in muscular dystrophies [49–52]. In the presented study, expression of Atrogin-1 and MuRF1 in LGMDR9 muscle biopsies did not differ from the control samples. Moreover, there was no apparent correlation between the levels of Atrogin-1 and

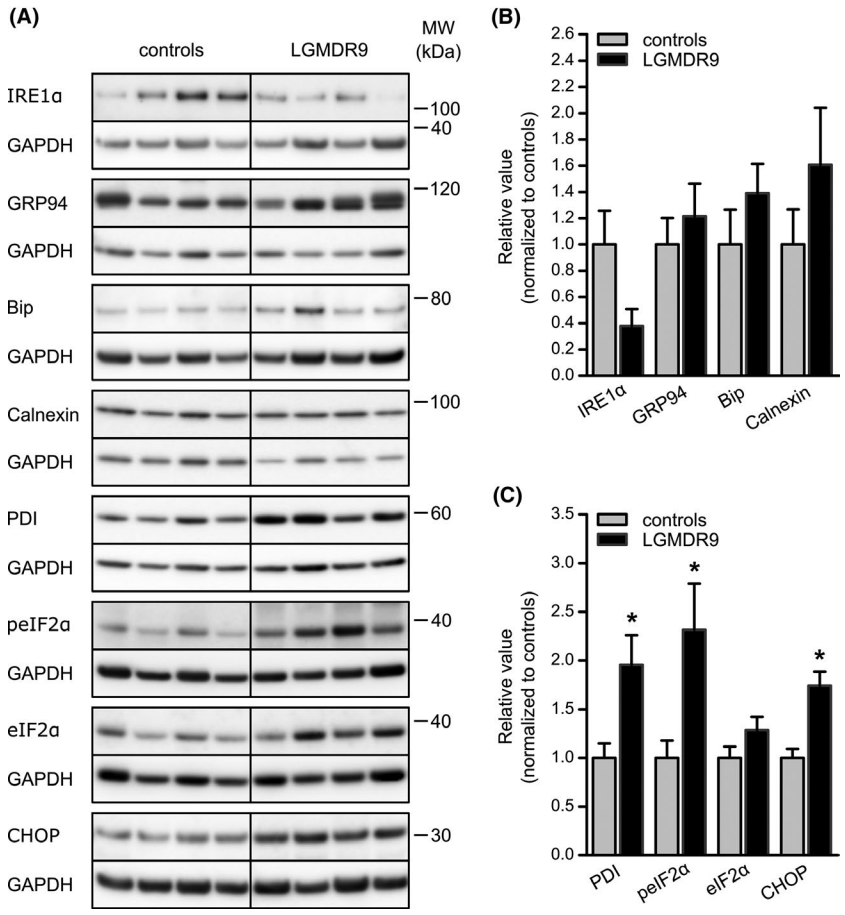

FIGURE 8 ER stress/UPR in LGMDR9 muscle. (A) Representative immunoblot analyses of muscle biopsies for IRE1α, Grp94, Bip, Calnexin, PDI, phospho-Ser51-eIF2α (peIF2α), eIF2α, CHOP and the loading control GAPDH from normal controls and LGMDR9 patients. (B) Densitometric quantification of the signals from immunoblot analyses corrected for loading control. Quantifications correspond to 8 normal controls and 12 LGMDR9 patients. Results are represented as mean values ±SEM and normalized to normal controls $^*p < 0.05$ vs. normal controls

MuRF1 expression and the grade of myofibre atrophy in LGMDR9 muscle biopsies presented in this work. Therefore, our data suggest that the atrophy observed in LGMDR9 is likely not to be caused by upregulation of the E3 ubiquitin ligases MuRF1 and Atrogin-1. However, the involvement of other UPS-associated E3 ligases, such as TRIM32, MUSA1 and NEDD4-1, cannot be ruled out [16, 53]. Furthermore, it is important to point out that we possess no information concerning the kinetics of protein translation or decay of these ligases in LGMDR9 muscle. It has been previously reported that, under conditions of disuse, the mRNA levels of Atrogin-1 and MuRF1 rapidly increase for a relatively short period of time, and then return to baseline within 2 weeks, suggesting their potential involvement in the remodelling process [17]. Therefore, induction of these genes at early stages of LGMDR9 cannot be rejected. Although the levels of Atrogin-1 and MuRF1 were not changed in LGMDR9 muscle as compared to normal controls, increased level of total ubiquitin as well as higher content of 20S subunits may suggest enhanced rates of protein degradation. Alternatively, increased ubiquitin levels may result from decreased rates of protein deubiquitination. These questions remain to be elucidated.

Autophagy markers and TEM indicate enhancement of autophagy in LGMDR9 muscle

To examine if autophagy is activated in skeletal muscle from patients with LGMDR9, markers of autophagosome formation and maturation were assessed by Western blot analysis, followed by ultrastructural examination of longitudinal muscle sections by TEM. Western blot data demonstrated significant increase in the expression of autophagy markers Atg7 and LC3B-II and TEM images displayed morphological alterations not ordinarily found in normal muscle. These included the appearance of autophagosome-like vacuoles and multi-lamellar bodies, strongly indicating ongoing autophagic processes [54]. In line with these data, rimmed vacuoles, which are thought to represent accumulation of autophagic vacuoles, have previously been reported in LGMDR9 muscle fibres [55-57]. The results from TEM were in accordance with increased abundance of autophagic markers and co-localization of LC3B with p62 and LAMP2, as measured by immunofluorescence analyses of LGMDR9 muscle. Accumulation of autophagosomes could be a consequence of increased autophagic flux or decreased

autophagosome clearance (e.g. dysfunction of autophagosome–lysosome fusion or autolysosome function). However, the increased levels of LC3B-II and Atg7, accompanied with reduction in p62 levels, indicate autophagy induction rather than autophagy blockage in LGMDR9 muscle. This notion was in line with the normal levels of lysosomal marker LAMP2, as well as significantly reduced phosphorylation of mTORC1 (Ser2448) and GSK3β (Ser9) in LGMDR9 muscle, as compared to normal controls.

However, we recognize that our data represent a static measurement of autophagic activity and cannot provide information about the movement of cargo through the autophagy pathway. Therefore, although the data presented here strongly support the idea of autophagy induction, rather than autophagy blockage, autophagy flux experiments *in vitro* would provide additional and important information in order to clarify whether autophagy is activated or hampered in skeletal muscle of LGMDR9 patients.

No correlation was observed between the expression levels of autophagy markers and the disease duration at biopsy or the degree of atrophy in LGMDR9 patients. This might suggest that autophagy proceeds independently of disease progression in these patients. However, more studies specifically designed to tackle this issue would be needed to confirm this hypothesis.

Mitophagy in LGMDR9 muscle

Mitophagy is a two-step process characterized by the induction of general autophagy followed by priming of the damaged mitochondria for mitophagic recognition and elimination [30]. Hence, since autophagy signalling is generally upregulated in LGMDR9 muscle, one would expect that this would enhance the induction of mitophagy. This notion is consistent with the observation of mitochondria enveloped in autophagic vacuoles as seen by TEM (Figure 4E). However, decreased expression levels of mitophagy markers Bnip3 and Parkin in LGMDR9 muscle indicate deficiency in this degradation process rather than its activation. This would be in line with the observed accumulation of swollen mitochondria and mitochondria without cristae which normally would be removed by mitophagy. On the other hand, this cannot explain the presence of areas lacking mitochondria in muscle fibres of some LGMDR9 patients. Furthermore, importantly, it should be noted that there exists a multitude of adaptors and substrates related to mitophagy, of which many function independently of the PINK1/Parkin pathway [58].

Notably, Parkin in LGMDR9 muscles demonstrated a shift in molecular mass of approximately 10 kDa, which potentially could correspond to the addition of mono-ubiquitin. However, whether such modification of Parkin would affect mitophagy in LGMDR9 muscle remains to be investigated.

Accumulation of abnormal mitochondria is associated with oxidative stress and increased production of reactive oxygen species (ROS). Increase in ROS is known to be involved not only in induction of apoptosis [59] but also in positive regulation of autophagy [60]. This opens for a pathway in which induction of autophagy in LGMDR9 muscle could be stimulated by ROS. Moreover, increased levels of ROS might explain the decreased level of anti-apoptotic Bcl2 and increased pro-apoptotic Bax.

ER stress is induced in LGMDR9 muscle

Dysfunction of ER has been suggested to play a significant role in several muscular dystrophies. Expression of ER stress markers has been shown to be increased in DMD, Myotonic dystrophy and Tibial muscular dystrophy (reviewed in [61]). Since ER stress can induce autophagy to participate in the degradation of unfolded proteins and in the removal of superfluous ER membranes, [44, 62] we investigated if markers of UPR were changed in LGMDR9 muscle.

Skeletal muscle from LGMDR9 patients reported herein showed significant changes in some (i.e. PDI, peIF2α, CHOP and IRE1α) but not all UPR markers. While there is a possibility that the expression of these proteins may also be governed through mechanisms independent of the ER stress response, ultrastructural changes in the sarcoplasmic reticulum seen in most of our LGMDR9 samples support the notion of increased ER stress in LGMDR9. Moreover, evidence of enhanced ER stress/UPR in LGMDR9 has previously been reported [63]. These authors found increased mRNA expression of GRP78 and CHOP, and furthermore, rough endoplasmic reticulum proliferation, dilated SR cisternae, triad reduplication as well as high numbers of lipid droplets in skeletal muscle of patients with LGMDR9. Similar features were observed in the present study, although the level of lipid droplets in our collection of LGMDR9 muscle biopsies was not to the extent as that reported in [63]. ER stress/UPR activation was also demonstrated in an *FKRP* knock-down Zebrafish model [64]. However, these alterations were not detected upon examination muscle samples from dystroglycanopathy patients with mutations in *FKRP*. The timing at which biopsies were obtained and/or the suitability of muscle tissue for measurement of changes in ER stress/UPR were suggested by authors as the potential factors causing the differences between the Zebrafish model and human patient samples [64].

The results presented here indicate ER stress in LGMDR9 muscle. However, the question concerning its activation as well as the mechanisms by which ER stress would invoke autophagy in LGMDR9 still remain elusive and require further investigation.

Summary

By means of *vastus lateralis* biopsies derived from patients with LGMDR9, we have investigated the pathological mechanisms underlying muscle wasting in this disorder. Our results show that activation of atrophy in LGMDR9 appears to be independent of the activation of E3 ubiquitin ligases, Atrogin-1 and MuRF1. Skeletal muscle of LGMDR9 patients has a protein expression profile that is concordant with enhanced autophagy and induction of ER stress.

These conclusions are supported by ultrastructural alterations seen on TEM images. However, more experiments are needed to clarify the regulatory mechanisms and to determine if these catabolic pathways would be suitable for therapeutic intervention in LGMDR9.

ACKNOWLEDGMENTS

We thank Kenneth B. Larsen and Randi Olsen from the Advanced Microscopy Facility (AMCF), Department of Medical Biology, UiT The Arctic University of Norway, Tromsø, Norway for their technical assistance. We also thank Peter Franek for assisting the preparation and layout figures.

CONFLICT OF INTEREST

No conflicts of interest, financial or otherwise, are declared by the authors.

AUTHOR CONTRIBUTIONS

VF and ØN designed the study, VF performed experiments, HS and VF performed TEM analysis, VF and ØN analysed data and interpreted results of experiments, VF drafted manuscript and prepared figures, VF, GL and ØN edited manuscript, VF, HS, GL and ØN read and approved the final version of manuscript.

ETHICAL APPROVAL

All patient biopsies were obtained with written informed consent and the study was approved by The Regional Committee for Medical Research Ethics (REK Nord) (REK# 159/207, 12/2008). With authorization in the ACT 2008–06–20 no.44: the Health Research Act, § 20, REK Nord waived the need for consent (REK# 2013/912) for anonymized normal biopsies from the local biobank (REK# 11/2008).

DATA AVAILABILITY STATEMENT

The data that support the findings of this study are available from the corresponding author upon reasonable request.

ORCID

Veronika Franekova https://orcid.org/0000-0001-8128-0259

REFERENCES

1. Brockington M. Mutations in the fukutin-related protein gene (FKRP) identify limb girdle muscular dystrophy 2I as a milder allelic variant of congenital muscular dystrophy MDC1C. *Hum Mol Genet*. 2001;10:2851-2859
2. Brockington M, Blake DJ, Prandini P, et al. Mutations in the fukutin-related protein gene (FKRP) cause a form of congenital muscular dystrophy with secondary laminin α2 deficiency and abnormal glycosylation of α-dystroglycan. *Am J Hum Genet*. 2001;69:1198-1209
3. Gerin I, Ury B, Breloy I, et al. ISPD produces CDP-ribitol used by FKTN and FKRP to transfer ribitol phosphate onto α-dystroglycan. *Nat Commun*. 2016;7:11534
4. Kanagawa M, Kobayashi K, Tajiri M, et al. Identification of a post-translational modification with ribitol-phosphate and its defect in muscular dystrophy. *Cell Rep*. 2016;14:2209-2223
5. Beltran-Valero de Bernabé D, Voit T, Longman C, et al. Mutations in the FKRP gene can cause muscle-eye-brain disease and Walker-Warburg syndrome. *J Med Genet*. 2004;41:e61–e61.
6. Poppe M, Cree L, Bourke J, et al. The phenotype of limb-girdle muscular dystrophy type 2I. *Neurol*. 2003;60:1246-1251.
7. Sveen M-L, Thune JJ, Køber L, et al. Cardiac involvement in patients with limb-girdle muscular dystrophy type 2 and becker muscular dystrophy. *Arch Neurol*. 2008;65:1196-1201.
8. Sveen ML, Schwartz M, Vissing J. High prevalence and phenotype-genotype correlations of limb girdle muscular dystrophy type 2I in Denmark. *Ann Neurol*. 2006;59:808-815.
9. Stensland E, Lindal S, Jonsrud C, et al. Prevalence, mutation spectrum and phenotypic variability in Norwegian patients with Limb Girdle Muscular Dystrophy 2I. *Neuromuscul Disord*. 2011;21:41-46.
10. Schwartz M, Hertz JM, Sveen ML, et al. LGMD2I presenting with a characteristic Duchenne or Becker muscular dystrophy phenotype. *Neurol*. 2005;64:1635-1637.
11. Mercuri E, Brockington M, Straub V, et al. Phenotypic spectrum associated with mutations in the fukutin-related protein gene. *Ann Neurol*. 2003;53:537-542.
12. Sandri M. Protein breakdown in muscle wasting: role of autophagy-lysosome and ubiquitin-proteasome. *Int J Biochem Cell Biol*. 2013;45:2121-2129
13. Murton AJ, Constantin D, Greenhaff PL. The involvement of the ubiquitin proteasome system in human skeletal muscle remodelling and atrophy. *Biochim Biophys Acta - Mol Basis Dis*. 2008;1782:730-743.
14. Bodine SC, Latres E, Baumhueter S, et al. Identification of ubiquitin ligases required for skeletal Muscle Atrophy. *Science (80-)* 2001;294:1704-1708.
15. Gomes MD, Lecker SH, Jagoe RT, et al. Atrogin-1, a muscle-specific F-box protein highly expressed during muscle atrophy. *Proc Natl Acad Sci USA*. 2001;98:14440-14445.
16. Rom O, Reznick AZ. The role of E3 ubiquitin-ligases MuRF-1 and MAFbx in loss of skeletal muscle mass. *Free Radic Biol Med*. 2016;98:218-230.
17. Bodine SC, Baehr LM. Skeletal muscle atrophy and the E3 ubiquitin ligases MuRF1 and MAFbx/atrogin-1. *Am J Physiol - Endocrinol Metab* 2014;307:E469-E484.
18. Autophagy MN. Process and function. *Genes Dev*. 2007;21:2861-2873.
19. Youle RJ, Narendra DP. Mechanisms of mitophagy. *Nat Rev Mol Cell Biol*. 2011;12:9-14.
20. Mizushima N, Levine B, Cuervo AM, et al. Autophagy fights disease through cellular self-digestion. *Nature* 2008;451:1069-1075.
21. Masiero E, Agatea L, Mammucari C, et al. Autophagy is required to maintain muscle mass. *Cell Metab*. 2009;10:507-515.
22. Masiero E, Sandri M. Autophagy inhibition induces atrophy and myopathy in adult skeletal muscles. *Autophagy* 2010; 6: 307-309.
23. Sandri M. New findings of lysosomal proteolysis in skeletal muscle. *Curr Opin Clin Nutr Metab Care* 2011;14:223-229.
24. Neel BA, Lin Y, Pessin JE. Skeletal muscle autophagy: A new metabolic regulator. *Trends Endocrinol Metab*. 2013;24:635-643
25. Sandri M, Coletto L, Grumati P, et al. Misregulation of autophagy and protein degradation systems in myopathies and muscular dystrophies. *J Cell Sci*. 2013;126:5325-5333.
26. Castets P, Frank S, Sinnreich M, et al. 'Get the Balance Right': pathological significance of autophagy perturbation in neuromuscular disorders. *J Neuromuscul Dis*. 2016;3:127-155.
27. Rasmussen M, Scheie D, Breivik N, et al. Clinical and muscle biopsy findings in Norwegian paediatric patients with limb girdle muscular dystrophy 2I. *Acta Paediatr Int J Paediatr*. 2014;103:553-558.
28. Alhamidi M, Brox V, Stensland E, et al. Limb girdle muscular dystrophy type 2I: No correlation between clinical severity, histopathology and glycosylated α-dystroglycan levels in patients

homozygous for common FKRP mutation. *Neuromuscul Disord*. 2017;27:619-626.
29. Kim I, Rodriguez-Enriquez S, Lemasters JJ. Selective degradation of mitochondria by mitophagy. *Arch Biochem Biophys*. 2007;462:245-253.
30. Ding WX, Yin XM. Mitophagy: mechanisms, pathophysiological roles, and analysis. *Biol Chem*. 2012;393:547-564.
31. Bonaldo P, Sandri M. Cellular and molecular mechanisms of muscle atrophy. *DMM Dis Model Mech*. 2013;6:25-39.
32. Mammucari C, Milan G, Romanello V, et al. FoxO3 controls autophagy in skeletal muscle in vivo. *Cell Metab*. 2007;6:458-471.
33. Zhao J, Brault JJ, Schild A, et al. FoxO3 coordinately activates protein degradation by the Autophagic/Lysosomal and proteasomal pathways in atrophying muscle cells. *Cell Metab*. 2007;6:472-483.
34. Wullschleger S, Loewith R, Hall MN. TOR signaling in growth and metabolism. *Cell* 2006; 124: 471-484.
35. Laplante M, Sabatini DM. MTOR signaling in growth control and disease. *Cell* 2012;149:274-293.
36. Cross DAE, Watt PW, Shaw M, et al. Insulin activates protein kinase B, inhibits glycogen synthase kinase-3 and activates glycogen synthase by rapamycin-insensitive pathways in skeletal muscle and adipose tissue. *FEBS Lett*. 1997;406:211-215.
37. Jiang H, Xiao J, Kang BO, et al. PI3K/SGK1/GSK3β signaling pathway is involved in inhibition of autophagy in neonatal rat cardiomyocytes exposed to hypoxia/reoxygenation by hydrogen sulfide. *Exp Cell Res*. 2016;345:134-140.
38. Kim J, Kundu M, Viollet B, et al. AMPK and mTOR regulate autophagy through direct phosphorylation of Ulk1. *Nat Cell Biol*. 2011;13:132-141
39. Sanchez AMJ, Csibi A, Raibon A, et al. AMPK promotes skeletal muscle autophagy through activation of forkhead FoxO3a and interaction with Ulk1. *J Cell Biochem*. 2012;113:695-710.
40. Paul PK, Gupta SK, Bhatnagar S, et al. Targeted ablation of TRAF6 inhibits skeletal muscle wasting in mice. *J Cell Biol*. 2010;191:1395-1411.
41. Paul PK, Bhatnagar S, Mishra V, et al. The E3 Ubiquitin Ligase TRAF6 intercedes in starvation-induced skeletal muscle atrophy through multiple mechanisms. *Mol Cell Biol*. 2012;32:1248-1259.
42. Axe EL, Walker SA, Manifava M, et al. Autophagosome formation from membrane compartments enriched in phosphatidylinositol 3-phosphate and dynamically connected to the endoplasmic reticulum. *J Cell Biol* 2008;182:685-701.
43. Razi M, Chan EYW, Tooze SA. Early endosomes and endosomal coatomer are required for Autophagy. *J Cell Biol*. 2009;185:305-321.
44. Ogata M, Hino S-I, Saito A, et al. Autophagy is activated for cell survival after endoplasmic reticulumstress. *Mol Cell Biol*. 2006;26:9220-9231.
45. Yorimitsu T, Nair U, Yang Z, et al. Endoplasmic reticulum stress triggers autophagy. *J Biol Chem*. 2006;281:30299-30304.
46. Høyer-Hansen M, Jäättelä M. Connecting endoplasmic reticulum stress to autophagy by unfolded protein response and calcium. *Cell Death Differ*. 2007;14:1576-1582.
47. Kouroku Y, Fujita E, Tanida I, et al. ER stress (PERK/eIF2α phosphorylation) mediates the polyglutamine-induced LC3 conversion, an essential step for autophagy formation. *Cell Death Differ*. 2007;14:230-239.
48. Hiramatsu N, Chiang W-C, Kurt TD, et al. Multiple mechanisms of unfolded protein response-induced cell death. *Am J Pathol*. 2015;185:1800-1808.
49. Carmignac V, Svensson M, Körner Z, et al. Autophagy is increased in laminin α2 chain-deficient muscle and its inhibition improves muscle morphology in a mouse model of MDC1A. *Hum Mol Genet*. 2011;20:4891-4902.
50. Paco S, Ferrer I, Jou C, et al. Muscle fiber atrophy and regeneration coexist in collagen VI-deficient human muscle: Role of calpain-3 and nuclear factor-κB signaling. *J Neuropathol Exp Neurol*. 2012;71:894-906.
51. Fanin M, Nascimbeni AC, Angelini C. Muscle atrophy in Limb Girdle Muscular Dystrophy 2A: a morphometric and molecular study. *Neuropathol Appl Neurobiol*. 2013;39:762-771.
52. Fanin M, Nascimbeni AC, Angelini C. Muscle atrophy, ubiquitin-proteasome, and autophagic pathways in dysferlinopathy. *Muscle Nerve* 2014;50:340-347.
53. Egerman MA, Glass DJ. Signaling pathways controlling skeletal muscle mass. *Crit Rev Biochem Mol Biol*. 2014;49:59-68.
54. Hariri M, Millane G, Guimond M-P, et al. Biogenesis of multilamellar bodies via autophagy. *Mol Biol Cell*. 2000;11:255-268.
55. Reilich P, Petersen JA, Vielhaber S, et al. LGMD 2I due to the common mutation 826C>A in the FKRP gene presenting as myopathy with vacuoles and paired-helical filaments. *Acta Myol*. 2006; 25: 73-76.
56. Yamamoto LU, Velloso FJ, Lima BL, et al. Muscle protein alterations in LGMD2I patients with different mutations in the fukutin-related protein gene. *J Histochem Cytochem*. 2008;56:995-1001.
57. Hong D, Zhang W, Wang W, et al. Asian patients with limb girdle muscular dystrophy 2I (LGMD2I). *J Clin Neurosci*. 2011;18:494-499.
58. Yoo SM, Jung YK. A molecular approach to mitophagy and mitochondrial dynamics. *Mol Cells* 2018;41:18-26.
59. Menazza S, Blaauw B, Tiepolo T, et al. Oxidative stress by monoamine oxidases is causally involved in myofiber damage in muscular dystrophy. *Hum Mol Genet*. 2010;19:4207-4215.
60. Scherz-Shouval R, Elazar Z. Regulation of autophagy by ROS: Physiology and pathology. *Trends Biochem Sci*. 2011;36:30-38.
61. Afroze D, Kumar A. ER stress in skeletal muscle remodeling and myopathies. *FEBS J*. 2019;286:379-398.
62. Bernales S, McDonald KL, Walter P. Autophagy counterbalances endoplasmic reticulum expansion during the unfolded protein response. *PLoS Biol*. 2006;4:2311-2324.
63. Boito CA, Fanin M, Gavassini BF, et al. Biochemical and ultrastructural evidence of endoplasmic reticulum stress in LGMD2I. *Virchows Arch*. 2007;451:1047-1055.
64. Lin Y-Y, White RJ, Torelli S, et al. Zebrafish fukutin family proteins link the unfolded protein response with dystroglycanopathies. *Hum Mol Genet*. 2011;20:1763-1775.

SUPPORTING INFORMATION

Additional supporting information may be found online in the Supporting Information section.

How to cite this article: Franekova V, Storjord HI, Leivseth G, Nilssen Ø. Protein homeostasis in LGMDR9 (LGMD2I) – The role of ubiquitin–proteasome and autophagy–lysosomal system. *Neuropathol Appl Neurobiol*. 2021;00:1–13. https://doi.org/10.1111/nan.12684